Tetrathiafulvalene Crowns: Redox-Switchable Ligands

Franck Le Derf,[a] Miloud Mazari,[a, e] Nicolas Mercier,[a] Eric Levillain,[a] Gaëlle Trippé,[a] Amédée Riou,[a] Pascal Richomme,[b] Jan Becher,[c] Javier Garín,[d] Jesus Orduna,[d] Nuria Gallego-Planas,[a] Alain Gorgues,[a] and Marc Sallé*[a]

Dedicated to Fred Wudl on the occasion of his 60th birthday

Abstract: A series of redox-responsive ligands that associate the electroactive tetrathiafulvalene core with polyether subunits of various lengths has been synthesized. X-ray structures are provided for each of the free ligands. The requisite structural criteria for reaching switchable ligands are satisfied for the largest macrocycles, that is, planarity of the 1,1',3,3'-tetrathiafulvalene (TTF) π system and correctly oriented coordinating atoms. The ability of these ligands to recognize various metal cations as a function of the cavity size has been investigated by various techniques (LSIMS, ^{1}H NMR, and UV/Vis spectroscopy, cyclic voltammetry). These systems exhibit an unprecedented high coordination ability among TTF crown ethers. Their switchable ligating properties have been confirmed by cyclic voltammetry, and metal-cation complexation has been illustrated by X-ray structures of three of the corresponding metal complexes (Pb^{2+}, Sr^{2+}, and Ba^{2+}). Solid-state structures of these complexes display original packing modes with channel-like arrangements.

Keywords: crown compounds · cyclic voltammetry · O ligands · solid-state structures · tetrathiafulvalenes

Introduction

In the case of a switchable ligand, recognition of a given guest compound is accompanied by a physico-chemical response (e.g. photo- or electrochemical). On the other hand, the binding constant of the host–guest complex may be modified by setting the same physical stimulus externally.[1] In this context, redox-responsive ligands have been widely explored, owing to their ability to give an electrochemical response upon complexation of a suitable guest molecule. In the case of metal-cation coordination, most complexes are built from the covalent association of a ligating subunit with an electroactive core, with the ferrocene moiety as the prototype.[1, 2] The strongly π-donating tetrathiafulvalene (TTF) core has recently appeared at the forefront of this topic,[3] as a result of its ability to allow sequential formation of two stable oxidized states ($TTF^{·+}$ and TTF^{2+}). Indeed, since the control of the association constants in redox-responsive ligands is essentially governed by electrostatic interactions, the tetrathiafulvalene moiety offers a unique opportunity to monitor not only the binding (neutral TTF) but also the progressive release of the metal cation ($TTF^{·+}$ and then TTF^{2+}).

These TTF-based macrocycles can be classified under model **A** or model **B** families, depending on the grafting sites of the crown and TTF subunits.

Model A   **Model B**   **Ia** (n=1)
                                  Ib (n=2)
                                  Ic (n=3)

Although most of the fused crown TTFs so far described are of model **A**, very few metal complexation studies have been

[a] Prof. M. Sallé, Dr. F. Le Derf, Dr. M. Mazari, Dr. N. Mercier, Dr. E. Levillain, G. Trippé, Prof. A. Riou, Dr. N. Gallego-Planas, Prof. A. Gorgues
Laboratoire d'Ingénierie Moléculaire et Matériaux Organiques
UMR CNRS 6501, Université d'Angers
2 Boulevard Lavoisier, 49045 Angers (France)
Fax: (+33)2-41-73-54-05
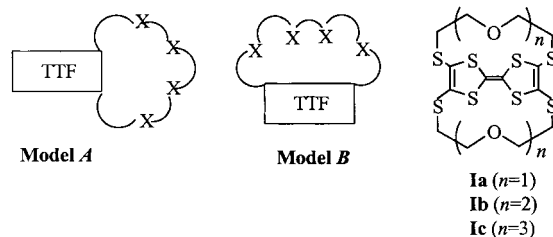E-mail: marc.salle@univ-angers.fr

[b] Prof. P. Richomme
SC RMN, Université d'Angers
2 Boulevard Lavoisier, 49045 Angers (France)

[c] Prof. J. Becher
Department of Chemistry, Odense University
Campusvej 55, 5230 Odense M (Denmark)

[d] Prof. J. Garín, Dr. J. Orduna
Instituto de Ciencia de Materiales de Aragon
Unidad de Nuevos Materiales Orgánicos, Facultad de Ciencias
CSIC-Universidad de Zaragoza, 50009 Zaragoza (Spain)

[e] Dr. M. Mazari
Laboratoire de Synthèse Organique Appliquée
Université d'Oran Es-Sénia, BP 1524, Oran (Algeria)

Supporting information for this article is available on the WWW under http://www.wiley-vch.de/home/chemistry/ or from the author.

carried out on these systems. When performed, these studies reveal, in the better cases, a limited electrochemical response, which is furthermore observed only in the presence of a large excess of metal cation. Such behavior may be explained by a low metal-binding ability and/or by a lack of communication between complexing and redox subunits.

On the other hand, the biggest HOMO coefficients of the TTF core are mainly located on the central $S_2C=CS_2$ fragment.[4] Therefore, model **B** receptors, whose complexing cavity is located in close spatial proximity to the TTF center, should be more appropriate for enhancing through-space interactions between a guest cation and the electroactive core.

Nevertheless, none of the crown TTFs **I**, which are built according to model **B**, displays satisfactory binding abilities.[5a] The main reason for this limitation is again structural, since the lateral polyether chains are presumably too short in these cases to give a suitable cavity size for accepting a guest compound. Moreover, the strain imposed by a short linker induces severe bending of the TTF π system,[5a] and leads to the loss of the two reversible one-electron redox processes classically encountered for a free TTF unit. Another limitation of the study of compounds **I** comes from the synthetic pathway, since yields through the coupling route dramatically decrease for increasing chain length. Thus, the largest receptor **Ic** ($n = 3$) was originally obtained in a very low yield ($<1\%$); this precluded any metal binding study.[5a]

We recently made a preliminary report on the efficiency of crown ether TTF **3** in electrochemically sensing a barium cation.[3d] Here, we report on the synthesis of a series of polyoxaethylene-fused TTF receptors **1–3** that are designed to optimize the communication between the complexing and electroactive subunits (i.e., model **B**) and that incorporate long, flexible, lateral chains. An X-ray structural determination is provided for each of the receptors **1**, **2**, and **3**, and their ability to recognize various metal cations as a function of their cavity size has been investigated by various techniques (LSIMS, ^{1}H NMR, and UV/Vis spectroscopy, cyclic voltam-

Abstract in French: *Une famille de ligands électrochimiquement contrôlés, associant le cœur électroactif tétrathiafulvalène aux unités polyéthers complexantes de différentes longueurs, a été synthétisée. Les structures RX de chacun des ligands libres ont été résolues et répondent, pour les plus grands d'entre-eux, aux critères requis pour la modulation redox de la constante de complexation: planéité du système-π et atomes coordonnants correctement orientés vers le centre de la cavité. Leur aptitude à reconnaître des cations métalliques variés en fonction de la taille de la cavité a été étudiée par différentes techniques (LSIMS, RMN ^{1}H, UV/Vis, voltampérométrie cyclique); ces systèmes disposent de propriétés complexantes supérieures à celles des ligands TTF-couronnes déjà décrits. Leur aptitude à moduler la complexation a été confirmée par voltampérométrie cyclique et enfin, la coordination de cations métalliques est illustrée par les structures à l'état solide de trois complexes correspondants (Pb^{2+}, Sr^{2+} et Ba^{2+}). Les structures de ces complexes montrent des modes d'empilements originaux sous la forme de canaux.*

metry). Furthermore, X-ray structural determinations of the corresponding metal complexes (Pb^{2+}, Sr^{2+}, and Ba^{2+}) are provided in three cases.

Results and Discussion

Compounds **1–3** were prepared under high dilution conditions in DMF from the [1+1] cyclocondensation of the 2,6-bis(2-cyanoethylsulfanyl)-3,7-bis(methylthio)tetrathiafulvalene (**4**)[6] with ω-diiodopentaethyleneglycol (**5**)[7] in the presence of cesium hydroxide (Scheme 1). Thanks to this synthetic strategy, compounds **1–3** have been obtained in satisfactory yields, irrespective of the chain length (**1**: 50 %, **2**: 50 %, **3**: 55 %). Ligands **1**, **2**, and **3** were obtained as *Z/E* isomeric mixtures whose relative amounts were 40:60, 80:20, and 90:10 respectively (as shown by ^{1}H NMR spectroscopy in CDCl$_3$).
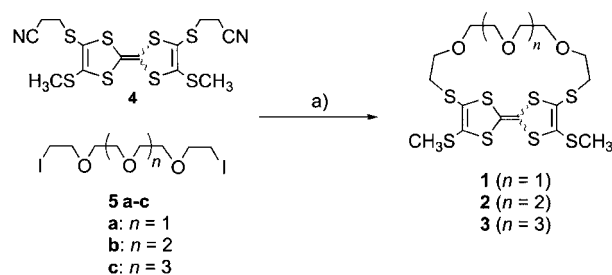
Scheme 1. a) DMF, CsOH, MeOH.

It is noteworthy that leaving the *Z/E* mixtures of the complexes in solution (CDCl$_3$, 20 °C, in the dark) for some days leads to new thermodynamic proportions, presumably through protonation of the central fulvalene C=C bond.[8] This isomerization can be monitored by ^{1}H NMR spectroscopy. Equilibrium is reached in a few days with new *Z/E* ratios of: 80:20 (**1**), 70:30 (**2**), and 70:30 (**3**). These values are in agreement with PM3 semiempirical calculations in which the geometry was optimized to obtain the total energy of each isomer (E_T). In compound **1**, the Z isomer was found to be significantly more stable than the E isomer: $\Delta E_T = 5.3$ kcal mol^{-1}. As expected, these calculations show that increasing the chain length tends to decrease the ΔE_T value between both isomers (**2**: $\Delta E_T = 2.6$ kcal mol^{-1}, **3**: $\Delta E_T = 1.8$ kcal mol^{-1}). Interestingly enough, pure (*Z*)-**2** could be obtained by fractional crystallization of the *Z/E* mixture (CH$_2$Cl$_2$/CH$_3$OH 1:9), even though no satisfactory chromatographic conditions could be found for efficient separation of the diastereoisomeric mixtures. Hence, we observed that CDCl$_3$ solutions of (*Z*)-**2** on the one hand and a mixture enriched with the (*E*)-**2** isomer (silica gel chromatography) on the other, both converge to the same thermodynamic ratio (*Z/E* 70:30) within a few days in the dark (Figure 1).

The structures of the crown TTFs **1–3** were established by two-dimensional NMR spectroscopy (DQF COSY, HMQC, HMBC). In the case of the macrocycle (*E*)-**1**, which has the shortest lateral chain of the series, the two protons of each
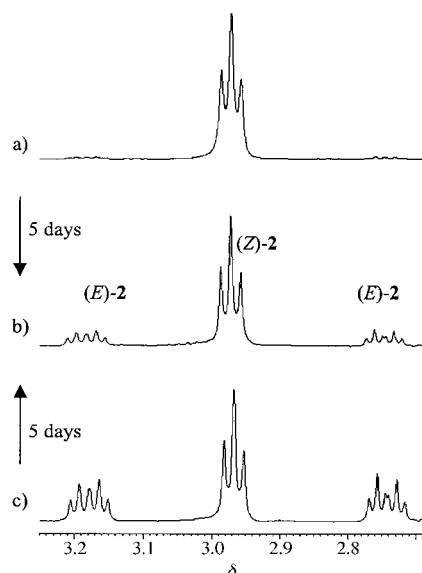
Figure 1. *Z/E* isomerization of compound **2** monitored by ¹H NMR (CDCl₃): a) (*Z*)-**2**, b) [(*Z*)-**2**/(*E*)-**2**] = (70:30), c) [(*Z*)-**2**/(*E*)-**2**] = (45/55).

methylene group of the SCH₂CH₂O fragments are not identical and give rise to an AA′BB′ system (see Experimental Section). This observation is in accordance with the expected low conformational mobility of the polyether bridge in (*E*)-**1** as compared with (*Z*)-**1**, for which the corresponding protons are identical; this results in two triplets. Macrocycle (*E*)-**2** behaves similarly to (*E*)-**1**, whereas these protons become equivalent in (*E*)-**3**, as expected from the higher internal mobility in the longer polyether chain.

The molecular structures of compounds **1–3** were confirmed by high resolution mass spectrometry and elemental analyses as well as by X-ray structural determinations in the case of (*E*)-**1**, (*Z*)-**2**, and (*Z*)-**3** (Figure 2 and Table 1). Single crystals were obtained by slow diffusion of pentane vapors on dichloromethanic solutions of the corresponding *Z/E* mixtures. They were obtained as orange-red crystals, this is to be expected for TTF derivatives with a good π delocalization, in contrast to the colorless crystals obtained in the case of the highly distorted TTF derivatives **I**.[5a]

As previously mentioned, the degree of planarity of the TTF core is a structural parameter of crucial importance in maintaining the redox properties (two reversible one-electron

processes) and, therefore, constitutes a prerequisite for reaching efficient electrochemically responsive ligands of the TTF family.

The bending angle (θ) of the TTF skeleton is defined as the average angle between the line C1=C2 on the one hand, and the plane incorporating S1, S2, C4, and C3 (or S3, S4, C6, and C5) on the other. Values of θ for (*E*)-**1**, (*Z*)-**2**, and (*Z*)-**3**, as well as those of compounds **I** for comparison, are given in Table 2.

Though it incorporates an additional CH₂CH₂O fragment, macrocycle (*Z*)-**2** has a similar θ value to (*E*)-**1**. On the other hand, the lengthening of the lateral polyether chain in going from (*Z*)-**2** to (*Z*)-**3** results in a marked decrease of the bending degree, with the TTF skeleton becoming quasi-planar in (*Z*)-**3** (θ = 5.1°). This results in a significant improvement compared with the value observed for compound **Ib** (θ = 34°), which corresponds to the largest model **B** crown-TTF assembly for which X-ray data are available.[5a, 9] Such a structural feature constitutes a crucial prerequisite, since the lack of conjugation in a nonplanar TTF skeleton leads to a lowering of the π-donating ability; this may even lead to the disappearance of the electrochemical reversibility (as in the case in **Ia**). This, of course, is incompatible with redox-sensing purposes. Indeed, we found that **1–3** exhibit the two classical reversible one-electron redox processes of TTF derivatives. The oxidation peak potentials of cage compounds **1–3** are nearly identical (Table 2) and are in the same range as those observed for the parent tetramethylsulfanyl TTF when recorded under similar conditions ($E_1^{ox} = 0.52$ V, $E_2^{ox} = 0.76$ V). Thus, MO calculations (PM3 method), which use the crystallographic data sets for (*E*)-**1**, (*Z*)-**2**, and (*Z*)-**3**, confirm these results, since all three macrocycles have similar HOMO energies (Table 2).

Another salient effect of the incorporation of long polyether chains in (*Z*)-**2** or (*Z*)-**3** lies in the large and flexible cavities used for complexation purposes that show appropriate orientation of the oxygen lone pairs toward the center of the cavity. In accordance with their relative number of CH₂CH₂O fragments, these cavities have dimensions of approximately 6.8 × 6.5 Å in the case of (*Z*)-**2** and 7.8 × 8.4 Å for (*Z*)-**3**.[10] Corey–Pauling–Kultun models showed that the *Z* isomers of **1–3** display the more suitable cavity geometries for complexation purposes. However, owing to the above-mentioned *Z/E* isomerization in solution, all complex-
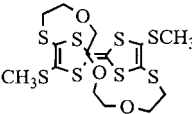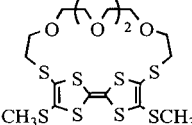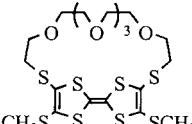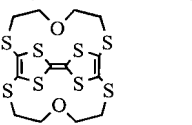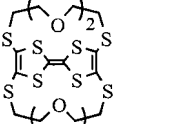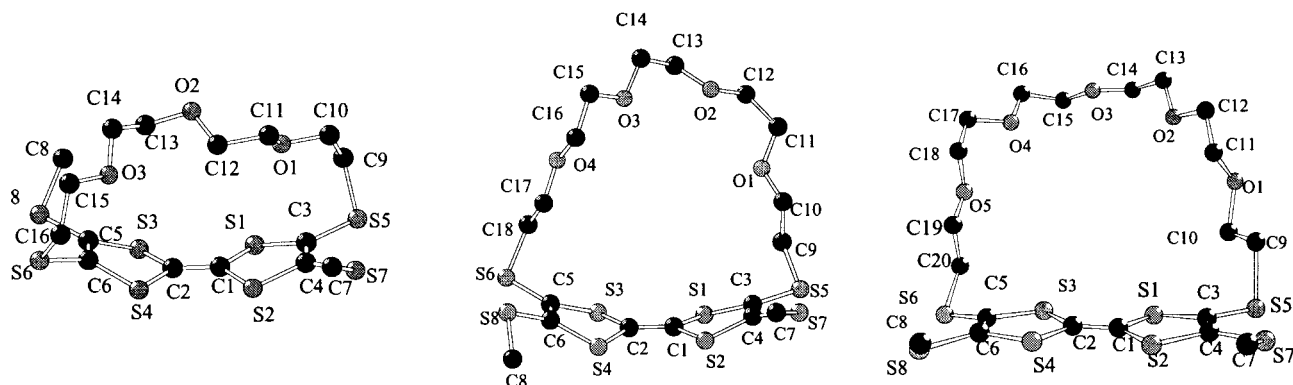

Figure 2. X-ray molecular structures of left: (*E*)-**1**, center: (*Z*)-**2**, right: (*Z*)-**3**.

Table 1. Crystallographic data for free ligands (E)-**1**, (Z)-**2**, and (Z)-**3** and corresponding complexes.

	(E)-**1**	(Z)-**2**	(Z)-**3**	[(Z)-**2**-Pb][(ClO₄)₂]· CD₃CN·H₂O	[(Z)-**2**-Sr][(ClO₄)₂]· CD₃CN·H₂O	[(Z)-**3**-Ba][(CF₃SO₃)₂]· CD₃CN·2H₂O
Formula	$C_{16}H_{22}O_3S_8$	$C_{18}H_{26}O_4S_8$	$C_{20}H_{30}O_5S_8$	$C_{20}H_{31}NO_{13}Cl_2S_8Pb$	$C_{20}H_{31}NO_{13}Cl_2S_8Sr$	$C_{24}H_{37}NO_{13}F_6S_{10}Ba$
M_w [Da]	518.86	562.92	606.97	1028.08	908.50	1119.53
color	orange	yellow	red	brown	brown	brown
crystal system	monoclinic	monoclinic	triclinic	triclinic	triclinic	monoclinic
Z	$(P2_1/c)/4$	$(P2_1/c)/4$	$(P\bar{1})/2$	$(P\bar{1})/2$	$(P\bar{1})/2$	$(C2/c)/8$
T [K]	293	293	293	293	293	293
a [Å]	11.609(4)	13.114(3)	9.087(6)	8.389(5)	8.42(2)	45.66(1)
b [Å]	13.37(1)	23.621(6)	11.637(7)	12.684(4)	12.70(1)	8.897(5)
c [Å]	15.300(7)	8.143(3)	14.370(8)	17.481(7)	17.44(5)	23.124(8)
α [°]	90	90	65.54(3)	88.06(3)	87.8(1)	90
β [°]	105.82(2)	90.28(2)	82.32(5)	78.43(4)	78.6(2)	105.54(4)
γ [°]	90	90	84.18(6)	88.36(3)	87.8(1)	90
V [Å³]	2284(3)	2522(2)	1368(1)	1820(4)	1828(8)	9050(10)
ρ_{calcd} [g cm⁻³]	1.32	1.48	1.47	1.88	–	1.64
μ [cm⁻¹]	5.8	7.03	6.55	53.1	–	13.95
$2\theta_{max}$	20	25	23	25	–	21
reflections	2333	4559	3727	6344	–	5354
independent reflns [$I > 3\sigma(I)$]	1393	1868	1665	3542	–	2062
parameters	244	271	298	406	–	301
R/Rw (|F|)[a]	0.062/0.080	0.053/0.070	0.056/0.077	0.060/0.092	–	0.103/0.118
$\Delta\rho$(max/min) [e − / Å⁻³]	0.83/ − 0.90	1.56/ − 1.08	1.06/ − 0.71	4.9/ − 1.33	–	2.43/ − 2.33

[a] $R = \dfrac{\sum (|F_o| - Z_k|F_c|)}{\sum |F_o|}$ $R_w = \dfrac{\sum w^{\frac{1}{2}}(|F_o| - Z_k|F_c|)}{\sum w^{\frac{1}{2}}|F_o|}$

Table 2. Oxidation potentials and bending angles obtained from X-ray data.

	θ [deg][a]	HO [eV][b]	$E_1^{ox[c]}$	$E_2^{ox[c]}$
(E)-**1**	25.6	− 8.18	0.50	0.72
(Z)-**2**	26.5	− 8.11	0.52	0.75
(Z)-**3**	5.1	− 8.12	0.53	0.73
Ia[5]	52	− 9.02	1.26[d]	–
Ib[5]	34	− 8.74	0.41[d]	0.73[d]

[a] TTF skeleton bending angle. [b] PM3 from X-ray data. [c] Peak potentials for compounds **1** – **3**: CH₂Cl₂/CH₃CN (1:1), Bu₄NPF₆ (0.1 mol L⁻¹), 100 mV s⁻¹, vs Ag/AgCl. [d] 1,1,2-trichloroethane, Bu₄NClO₄ (0.1 mol L⁻¹) 120 mV s⁻¹, vs Ag/AgCl.[5b]

ation studies were performed on diastereoisomeric mixtures. Whereas no cation coordination properties were found for the smaller TTF cage **1** whatever the investigation methods used (MS, ¹H NMR spectroscopy, cyclic voltammetry), evidence

for metal-cation recognition of hosts **2** and **3** initially came from LSIMS studies.

The addition of increasing amounts of Sr(ClO₄)₂ to crown ether **2** resulted in the formation of a 1:1 complex (m/z 749 [(Z)-**2**-Sr(ClO₄)]⁺, 848 [(Z)-**2**-Sr(ClO₄)₂]⁺) in the mass spectrum (nitro benzyl alcohol; mNBA). In contrast, no significant evidence of complexation was noticed in the presence of other metallic cations of Groups 1 or 2. The Sr²⁺ binding affinity of (Z)-**2** was evaluated by measuring the peak intensity of the host – guest complex (m/z 749), normalized to the m/z 307 peak of the mNBA matrix, with a progressive increase in the metal concentration.[3c, 3d, 11] Figure 3 shows a plot of the
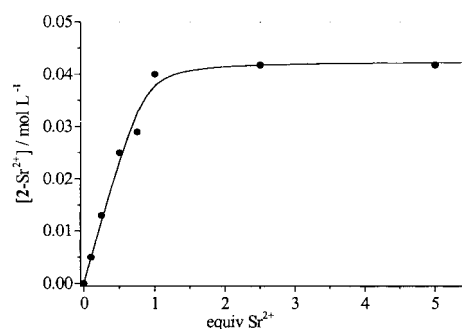
Figure 3. LSI MS (NBA matrix) titration of ligand **2** (C = 0.05 mol L⁻¹) with Sr(ClO₄)₂.

complex concentration as a function of the amount of metallic cation added. A plateau is observed for an excess of added Sr²⁺. This plateau corresponds to a concentration of about 0.040 mol L⁻¹ of complex or to 80% of the total amount of crown ether TTF **2** (Z + E). This result, along with the 80:20 (Z/E) ratio determined for receptor **2** (NMR spectrocopy), confirms that Sr²⁺ is trapped by the Z isomer only. Calculation

of the binding constant was carried out with a curve-fitting program, and gave a $\log K°$ value of 2.8 for the (Z)-**2**-Sr^{2+} complex.

As expected, the metal-binding properties of these systems are dependent on their cavity size, as shown by the strong affinity of ligand **3** for Ba^{2+} (i.e., the following element in the alkaline-earth group: m/z 843 [(Z)-**3**-Ba(ClO$_4$)]$^+$, 942 [(Z)-**3**-Ba(ClO$_4$)$_2$]$^+$; $\log K° = 3.5$, mNBA).[3d]

This observation is confirmed by ^{1}H NMR titration experiments carried out on cages **2** and **3** in the presence of various metallic cations. Thus, the complexation ability of receptor **2** in the presence of Sr^{2+} could be evidenced by ^{1}H NMR spectroscopy by addition of Sr(ClO$_4$)$_2$ to a solution of the ligand in CDCl$_3$/CD$_3$CN (1:1). This study shows the crown ether methylene protons of (Z)-**2** ($\delta = 3.56$) to be shifted to lower field; this indicates that complexation takes place with the polyether fragment. Receptor **2** exhibits similar behavior in the presence of Pb(ClO$_4$)$_2$, an expected result when the very close Sr^{2+} and Pb^{2+} ionic radii values are considered.[12] The resulting titration curves (Figure 4) reach a plateau for about one equivalent of added cation relative to (Z)-**2**.
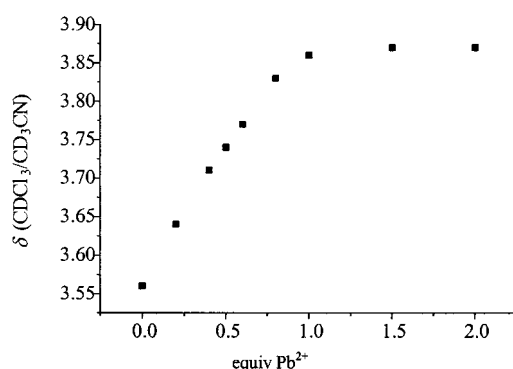

Figure 4. ^{1}H NMR titration curve of the perturbation of the CH$_2$O protons of ligand **2** on addition of Pb^{2+}.

Analysis of these data with the program EQNMR[13] suggested that the crown ether recognition site of (Z)-**2** forms a 1:1 complex with the strontium and lead cations, with stability constant values of $K° = 10^{3.4}$ (Sr^{2+}) and $K° = 10^{3.7}$ (Pb^{2+}).

Addition of Ba(CF$_3$SO$_3$)$_2$ to a solution of ligand **3** in CDCl$_3$/CD$_3$CN (1:1) resulted in an even higher $K°$ value of $10^{4.2}$ (NMR spectroscopy), which corresponds to the highest association constant so far observed with a TTF-based ligand. Accordingly, the good affinity of **3** for the barium cation was demonstrated by UV/Vis spectroscopy (CH$_2$Cl$_2$/CH$_3$CN 1:1), as shown in Figure 5. The isosbestic points at 322 and 382 nm provide alternative evidence for a 1:1 complex, and determination of the association constant by the Benesi–Hildebrand method[14] gave $K° = 10^{4.1}$ ($r = 0.999$).

Finally, the recognition properties of the redox-active receptors **1**–**3** were evaluated by cyclic voltammetry (CV) and square wave CV with the same medium (CH$_2$Cl$_2$/CH$_3$CN 1:1). Whereas no perturbation of the CV of crown TTF **1** was observed upon addition of Group 1 or 2 cations, significant modifications of the CVs of **2** and **3** could be observed upon addition of Sr^{2+} or Pb^{2+} cations, in the case of **2**, and Ba^{2+}
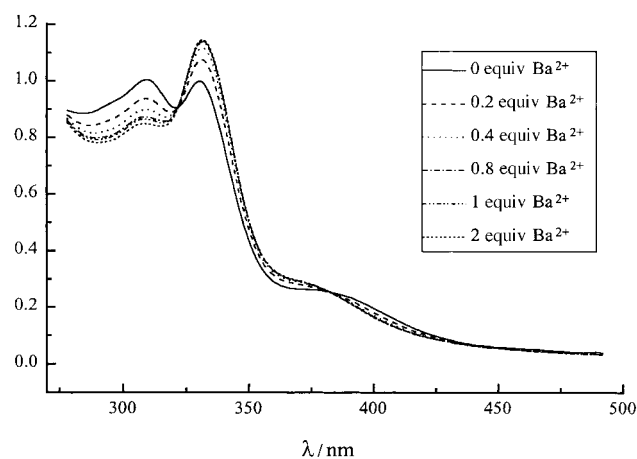

Figure 5. Absorption spectra of **3** (2.5×10^{-4} mol L^{-1} in CH$_2$Cl$_2$/CH$_3$CN 1:1) in the presence of increasing amounts of Ba^{2+}.

cations, in the case of **3**. This provides a further indication for the good complexation selectivity of these receptors.

Addition of a controlled amount of M(ClO$_4$)$_2$ (M = Sr or Pb) to a solution of cage TTF **2** in CH$_2$Cl$_2$/CH$_3$CN (1:1) with Bu$_4$NPF$_6$ (0.1 mol L^{-1}) caused substantial positive shifts ($\Delta E = 45$ and 60 mV respectively) of the first oxidation potential (E_1^{ox}), whereas E_2^{ox} remained unchanged (Figure 6, top).

A more important E_1^{ox} shift was observed on adding Ba(CF$_3$SO$_3$)$_2$ to receptor **3** ($\Delta E_1^{ox} = 100$ mV). In this case, a clearly distinguishable, new reversible wave appeared under thin layer cyclic voltammetry conditions; this indicates the stability of the barium complex thus formed (Figure 7).

The reason why the first oxidation wave is shifted to more anodic potentials is interpreted as being a result of the electrostatic inductive effect of the metal bound to crown ether withdrawing the electron density from the TTF moiety. Of course, the binding constants are expected to be lower in the radical-cation states than for neutral ligands, due to the TTF radical cation charge being in close proximity to the metallic cation.

On the other hand, the dicationic state of the TTF core is reached at a constant E_2^{ox} value, irrespective of the amount of metal cation added. This behavior can be explained by the expulsion of the metal cation from the cavity, owing to the increased repulsive electrostatic interaction with the doubly charged TTF moiety. Therefore, the present TTF ligands appear very attractive when compared with related ferrocene-based redox-responsive ligands, for which the monocharged, oxidized form does not allow full control of the metal-cation-expulsion process.

Interestingly, the E_1^{ox} shifts reach a limit when approximately stoichiometric amounts of Sr^{2+} or Pb^{2+} (or Ba^{2+}) are added to receptors **2** (or **3**). This result provides further evidence for the high stability of the 1:1 complexes and is in marked contrast to observations previously made on crown ether TTF derivatives for which a 250-fold excess of added metallic cation was necessary to get saturation of the system.[3a, b]

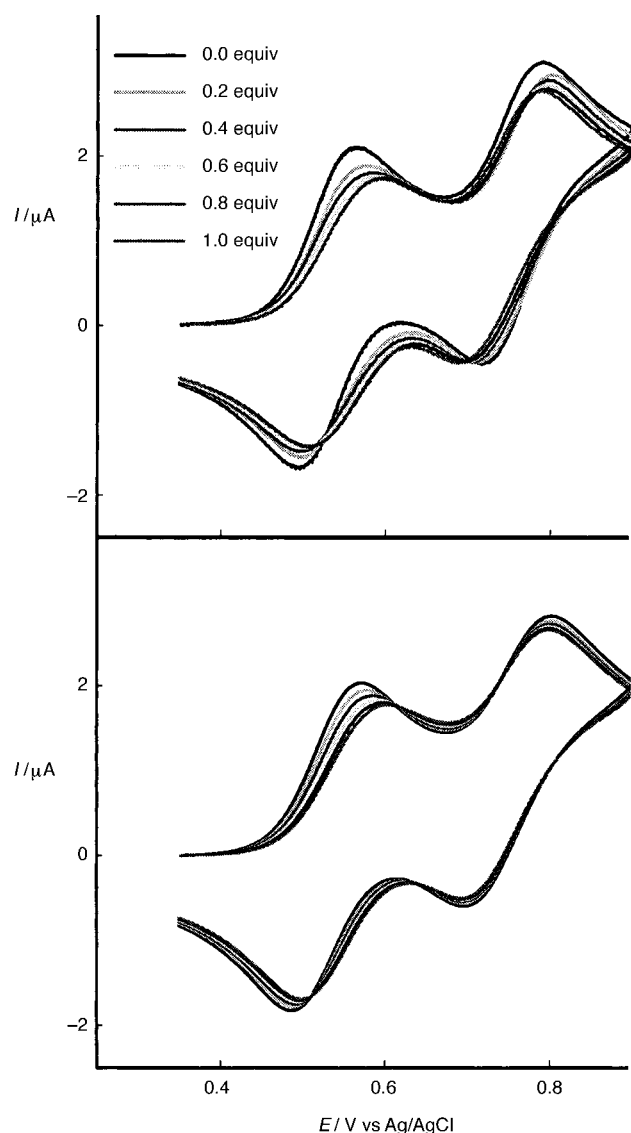Electrochemical modulation of the binding properties of ligands **2** and **3** was evaluated by the DIGISIM2.1®

Figure 6. Experimental (top) and simulated (bottom) cyclic voltammograms of compound **2** in the presence of increasing amounts of Pb^{2+}. The simulated data were fitted to experimental results for **2** (10^{-3} mol L^{-1} in CH$_2$Cl$_2$/CH$_3$CN 1:1) at 293 K and 100 mV s^{-1}. All simulations were carried out with the same set of parameters, except for the Pb^{2+} equivalent concentration, which was changed according to the experimental voltammograms. Charge transfer parameters: $k_s = 10^{-2}$ cm s^{-1} (free ligand **2**), $k_s = 0.1 \times 10^{-2}$ cm s^{-1} (**2**-Pb complex), $\alpha = 0.5$. Chemical reaction parameters: $K = 4250$ L mol^{-1}, $k_f^\circ = 10^6$ L mol^{-1} s^{-1}, and $K^{\cdot+} = 50$ L mol^{-1}, $k_f^{\cdot+} = 10^6$ L mol^{-1} s^{-1}. Diffusion coefficient: $D = 1.1 \times 10^{-5}$ cm^2 s^{-1}.

simulation program (BAS Inc.)[15] on the basis of a square scheme (see Figure 6, bottom).

The binding constant values of the different complexes are given in Table 3 as a function of the oxidation state of the electroactive TTF core in ligands **1**–**3** (K°, $K^{\cdot+}$, and K^{++} for TTF$^\circ$, TTF$^{\cdot+}$, and TTF^{2+}, respectively).

As expected, the binding constants are clearly dependent on the oxidation state of the redox-active TTF core. Hence, we found remarkably high K° values for the three complexes when compared with other TTF-based receptors described in the literature. An excellent convergence is found for the K° values of a given complex ([**2**-Pb]$^{2+}$: $K^\circ \approx 10^{3.6}$; [**2**-Sr]$^{2+}$:
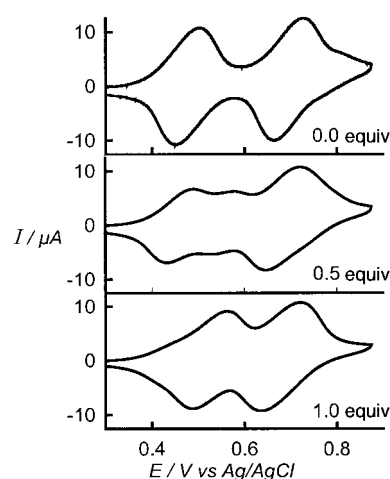

Figure 7. Thin-layer cyclic voltammetry of ligand **3** (10^{-3} mol L^{-1}) in the presence of increasing amounts of Ba^{2+}. CH$_2$Cl$_2$/CH$_3$CN 1:1, Bu$_4$NPF$_6$ (0.5 mol L^{-1}), $v = 2$ mV s^{-1}, electrode diameter = 5 mm.

Table 3. Association constants (K°, $K^{\cdot+}$, K^{2+}) for ligands **2** and **3** in the presence of metal cations.

		^{1}H NMR[a]	UV/Vis[b]	CV[b]			LSIMS (*m*NBA)
		K°	K°	K°	$K^{\cdot+}$	K^{2+}	K°
2	Sr^{2+}	$10^{3.4}$	–	$10^{3.4}$	$10^{2.1}$	0	$10^{2.8}$
2	Pb^{2+}	$10^{3.7}$	–	$10^{3.6}$	$10^{1.7}$	0	–
3	Ba^{2+}	$10^{4.2}$	$10^{4.1}$	$10^{4.3}$	$10^{2.4}$	0	$10^{3.5}$

[a] CDCl$_3$/CD$_3$CN, 1:1. [b] CH$_2$Cl$_2$/CH$_3$CN, 1:1.

$K^\circ \approx 10^{3.4}$; [**3**-Ba]$^{2+}$: $K^\circ \approx 10^{4.2}$), though they have been determined from techniques as different as ^{1}H NMR and UV/Vis spectroscopy, and cyclic voltammetry (Table 3); this underlines the complementarity of these methods, provided that the experiments are carried out in similar media.

Finally, slow diffusion of pentane vapors onto the above mentioned NMR titration solutions afforded crystals of the corresponding metal complexes (i.e. [(Z)-**2**-Pb]$^{2+}$, [(Z)-**2**-Sr]$^{2+}$, and [(Z)-**3**-Ba]$^{2+}$). X-ray structural determinations revealed the following stoichiometries: [(Z)-**2**-M][(ClO$_4$)$_2$] · CD$_3$CN · H$_2$O (M = Sr, Pb) (Figure 8) and [(Z)-**3**-Ba][(CF$_3$SO$_3$)$_2$] · CD$_3$CN · 2 H$_2$O[3d] (Table 1). To the best of our knowledge, these are the only known examples of TTF-ligand–metal complexes for which X-ray data are available. Though poorly resolved, the [(Z)-**2**-Sr]$^{2+}$ complex appears isostructural to the corresponding lead complex [(Z)-**2**-Pb]$^{2+}$ as a result of the almost identical ionic radii of octacoordinated Sr^{2+} and Pb^{2+} ($R_{Sr}^{2+} = 0.126$ nm, $R_{Pb}^{2+} = 0.129$ nm).[12]

In both cases, [(Z)-**2**-Pb]$^{2+}$ and [(Z)-**3**-Ba]$^{2+}$, the metallic cation is located in the center of the cavity. Interatomic bond lengths for the octa- and decacoordinated Pb^{2+} and Ba^{2+} complexes are given in Table 4.

Whereas only a minor modification of the bending of the TTF skeleton is observed in the complex [(Z)-**2**-Pb][(ClO$_4$)$_2$] · CD$_3$CN · H$_2$O ($\theta = 24.3°$) compared with the free ligand (Z)-**2** ($\theta = 26.5°$), coordination of the barium cation in (Z)-**3** induces a significant change ($\theta = 5.1°$ in (Z)-**3**, and $\theta = 29.6°$ in the complex).

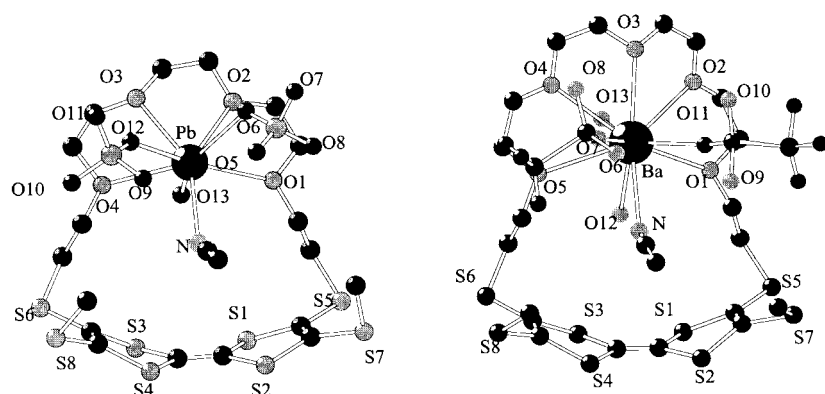Both Pb and Ba complexes crystallize according to a centrosymmetric arrangement. Interestingly, they give rise to

Figure 8. X-ray molecular structures of left: [(Z)-**2**-Pb][(ClO$_4$)$_2$] · CD$_3$CN · H$_2$O; and right: [(Z)-**3**-Ba][(CF$_3$SO$_3$)$_2$] · CD$_3$CN · 2H$_2$O.

Table 4. Coordination bond lengths [Å] in [(Z)-**2**-Pb][(ClO$_4$)$_2$] · CD$_3$CN · H$_2$O and [(Z)-**3**-Ba][(CF$_3$SO$_3$)$_2$] · CD$_3$CN · 2H$_2$O

[(Z)-**2**-Pb][(ClO$_4$)$_2$] · CD$_3$CN · H$_2$O		[(Z)-**3**-Ba][(CF$_3$SO$_3$)$_2$] · CD$_3$CN · 2H$_2$O	
Pb–O1	2.62(1)	Ba–O1	2.91(2)
Pb–O2	2.54(1)	Ba–O2	2.88(2)
Pb–O3	2.63(1)	Ba–O3	2.88(2)
Pb–O4	2.64(1)	Ba–O4	2.93(3)
Pb–O6	2.80(2)	Ba–O5	2.92(2)
Pb–O12	2.85(1)	Ba–O7	2.74(3)
Pb–O13	2.39(1)	Ba–O11	2.72(2)
Pb–N	2.76(2)	Ba–O12	2.87(3)
		Ba–O13	2.80(3)
		Ba–N	2.99(3)

packing modes in which the TTF core and the polyether subunit are stacked in a segregated way, in a channel-like arrangement with the cation in the center (Figure 9, Fig-
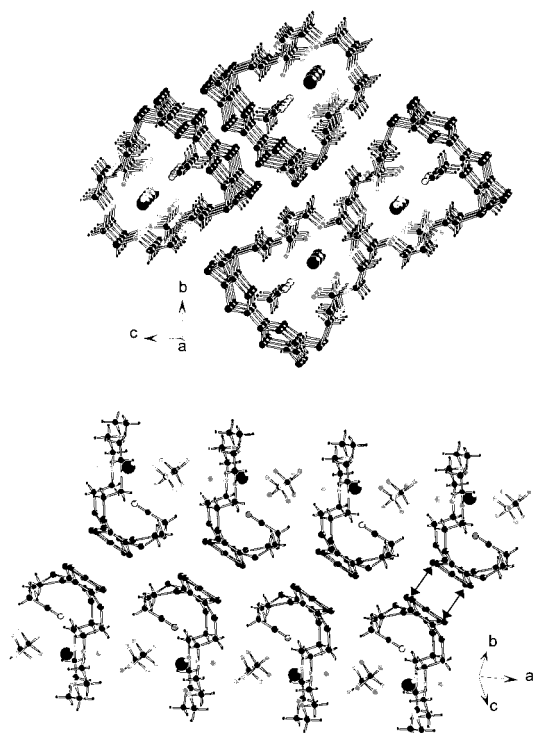
ure 10). The TTF planes are located face to face in the Pb complex with an interplanar distance of 3.55 Å, that is, a shorter distance than twice the van der Waals radius of the sulfur atom ($2r_{vdw} = 3.60$ Å). Similarly short S–S intermolecular distances (3.52 Å and 3.57 Å) are found for the barium complex, in which the TTF molecular planes in the electroactive layer are tilted away from each other with an angle of 45° along the b axis (Figure 10). There-
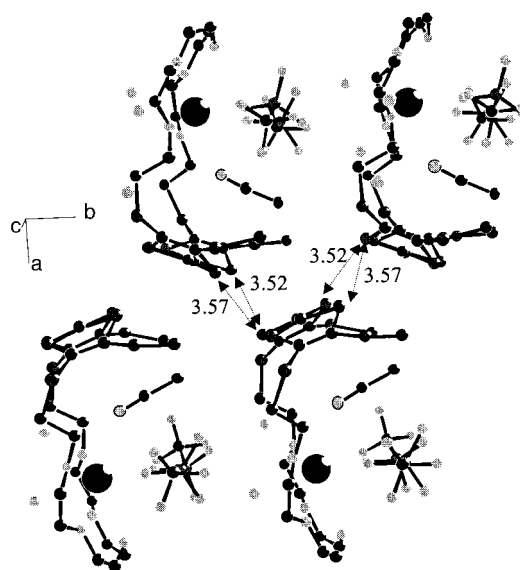

Figure 10. Intermolecular distances in [(Z)-**3**-Ba][(CF$_3$SO$_3$)$_2$] · CD$_3$CN · 2H$_2$O.

fore, this complex is obtained as a two-dimensional array in which electroactive (TTF) layers are separated by coordinating crown ether ones. This stacking mode is of great interest in connection with organic materials derived from the TTF family, for which it is well established that solid-state electroconductive properties are closely dependent on the overlaps between TTF units.[16] Additionally, great efforts are currently being devoted to the preparation of hybrid TTF materials that combine magnetism and conductivity.[17] In this context, the new metal–TTF-ligand complexes described here offer a unique opportunity in materials science, and preparation of similar complexes that associate transition metal cations with unpaired spins to an oxidized TTF ligand is in progress.

In conclusion, we have synthesized a series of TTF-based ligands that exhibit high coordination properties compared with previous systems of this family, both in terms of selectivity (correlated to their respective cavity sizes) and in terms of association-constant values. Their switchable ligating properties have been confirmed by cyclic voltammetry, and, finally, metal-cation complexation has been illustrated by the solid-state structures of three metal complexes.

Figure 9. Stacking mode of [(Z)-**2**-Pb][(ClO$_4$)$_2$] · CD$_3$CN · H$_2$O: top: view along the a axis; bottom: interplanar contacts.

Experimental Section

NMR spectra were recorded on a Bruker Advance DRX 500 spectrometer operating at 500 MHz and 125.7 MHz for ^{1}H and ^{13}C, respectively. δ values are given in ppm (relative to TMS) and J values in Hz. ^{1}H NMR titration experiments were carried out as follows (constant temperature: 22°C): seven NMR tubes were each filled with 15.0 mg of the ligand and an adequate amount of M^{2+} (i.e., 0, 0.25, 0.5, 0.75, 1, 2, and 5 equiv respectively), the total volume was then adjusted to 1 mL with CD$_3$CN/CDCl$_3$ (1:1 v/v). This solvent mixture proved to be the best compromise to solubilize both constituents (crown TTF and metal). Mass spectra were recorded on a VG-Autospec (Micromass, UK). EI mass spectra were obtained at 70 eV and accurate mass measurements were performed at 10 000 resolution (peak width at 5% height) with PFK (perfluorokerosene) as internal reference. LSI mass spectra were obtained by using the standard Cs$^+$ gun operated at 30 kV. For the determination of absolute binding constants, the spectra of solutions of **2** or **3** in NBA (2 μL, 0.05 M) which contained variable concentrations of Sr(ClO$_4$)$_2$ or Ba(ClO$_4$)$_2$, respectively, were recorded. Electrochemical experiments were carried out with a PAR 273 Potentiostat-Galvanostat in a three-electrode single-compartment cell equipped with platinum microelectrodes of area 7.85×10^{-3} cm^2, a platinum-wire counter electrode, and a Ag/AgCl reference electrode. Cyclic voltammetry was performed in methylene chloride/acetonitrile (1:1 v/v) solutions (SDS, HPLC grade), which contained tetrabutylammonium hexafluorophosphate (0.10 M; Fluka). Solutions were deaerated by argon bubbling prior to each experiment which was run under an inert atmosphere.

Synthetic procedure: **(*E,Z*)-3,6(7)-bis(methylsulfanyl)-2,7(6)-(4,7,10-tri-oxa-1,13-dithiatridecane-1,13-diyl) tetrathiafulvalene (1)**: A solution of cesium hydroxide (0.37 g, 2.2 mmol) in methanol (10 mL) was added at room temperature and under nitrogen to a stirred solution of compound **4** (0.466 g, 1 mmol) in dry DMF (50 mL). After stirring for 15 min, the resulting mixture and a solution of 1,11-diiodo-3,6,9-trioxaundecane (**5a**; 0.414 g, 1 mmol) in DMF (60 mL) were transferred separately under nitrogen into two syringes that were connected to a perfusor pump. The solutions were then added simultaneously and very slowly (5 mL h) under nitrogen and at room temperature into a round bottom flask containing DMF (200 mL). When addition was complete (12 h), the mixture was allowed to stir for three additional hours. The solvents were then evaporated in vaccuo. The oil obtained was dissolved in methylene chloride (50 mL), washed with water (3 × 50 mL), and dried over sodium sulfate. After evaporation, the residue was purified by chromatography on a silica gel column (methylene chloride/ethyl acetate 9:1). Evaporation of the solvents and precipitation in methanol afforded pure **1** as a bright orange solid. Yield: 0.26 g, 50%; (*Z*)-**1**/(*E*)-**1** = 2:3 (determined by ^{1}H NMR); ^{1}H NMR (500 MHz, CDCl$_3$, 25°C, TMS): δ = 3.81 (m, 2H; SCH$_2$CH_aO, *E*), 3.65 (t, 4H; SCH$_2$CH_2O, *Z*), 3.58 (m, 2H; SCH$_2$CH_bO, *E*), 3.49 (m, 8H; OCH$_2$CH$_2$O, *Z*), 3.46 – 3.33 (m, 8H; OCH$_2$CH$_2$O, *E*), 3.18 (m, 2H; SCH$_a$, *E*), 2.93 (t, 4H; SCH$_2$, *Z*), 2.72 (m, 2H; SCH$_b$, *E*), 2.41 (s, 6H; SCH$_3$, *E*), 2.38 (s, 6H; SCH$_3$, *Z*); ^{13}C NMR (125.7 MHz, CDCl$_3$, 25°C, TMS): δ = 131.8 (*E*), 130.1 (*Z*), 127.8 (*Z*), 126.8 (*E*), 114.8 (*E*), 113.2 (*Z*), 75.5 (*E*), 72.9 (*Z*), 72.4 (*E*), 71.7 (*E*), 71.6 (*Z*), 36.6 (*E*), 36.2 (*Z*), 20.3 (*Z*), 20.2 (*E*); MS (EI): [*M*]$^+$ calcd: 517.9335; found: 517.9347; elemental analysis calcd (%) for C$_{16}$H$_{22}$O$_3$S$_8$: C 37.07, H 4.28, O 9.26, S 49.38; found C 37.12, H 4.29, O 9.54, S 49.66.

[*E,Z*]-3,6(7)-bis(methylsulfanyl)-2,7(6)-(4,7,10,13-tetraoxa-1,16-dithiahexa-decane-1,16-diyl) tetrathiafulvalene (2): Crown ether TTF **2** was synthesized in a similar way to compound **1**, by using a solution of 1,14-diiodo-3,6,9,12-tetraoxatetradecane (**5b**). Compound **2** was obtained as a bright orange solid. Yield: 0.28 g, 50%; (*Z*)-**2**/(*E*)-**2** = 4:1 (determined by ^{1}H NMR); ^{1}H NMR (500 MHz, CDCl$_3$, 25°C, TMS): δ = 3.80 (m, 2H; SCH$_2$CH_aO, *E*), 3.57 (m, 2H; SCH$_2$CH_bO, *E*), 3.55 (s, 16H; CH$_2$O, *Z*), 3.55 – 3.48 (m, 12H; CH$_2$O, *E*), 3.18 (m, 2H; SCH$_a$, *E*), 2.98 (t, 4H; SCH$_2$, *Z*), 2.75 (m, 2H; SCH$_b$, *E*), 2.46 (s, 6H; SCH$_3$, *Z*), 2.44 (s, 6H; SCH$_3$, *E*); ^{13}C NMR (125.7 MHz, CDCl$_3$, 25°C, TMS): δ = 131.4 (*Z*+*E*), 126.5 (*Z*+*E*), 112.7 (*Z*), 112.0 (*E*), 72.2 (*E*), 72.1 (*E*), 71.9 (*Z*+*E*), 71.8 (*Z*), 71.4 (*Z*), 36.5 (*E*), 36.2 (*Z*), 20.2 (*Z*), 20.1 (*E*); MS (EI): [*M*]$^+$ calcd: 561.9597; found: 561.9605; elemental analysis calcd (%) for C$_{18}$H$_{26}$O$_4$S$_8$: C 38.44, H 4.66, O 11.39, S 45.52; found C 37.99, H 4.65, O 11.36, S 44.80.

(*E,Z*)-3,6(7)-bis(methylsulfanyl)-2,7(6)-(4,7,10,13,16-pentanoxa-1,19-di-thianonadecane-1,19-diyl) tetrathiafulvalene (3).[3d] Crown ether TTF **3** was synthesized in a similar way to compound **1**, by using a solution of 1,17-diiodo-3,6,9,12,15-pentaoxaheptadecane (**5c**). Compound **3** was obtained as a bright orange solid. Yield: 0.28 g, 50%; (*Z*)-**3**/(*E*)-**3** = 9:1 (determined by ^{1}H NMR); ^{1}H NMR (500 MHz, CDCl$_3$, 25°C, TMS): δ = 3.65 – 3.54 (m, 20H; CH$_2$O, *E*), 3.58 (s, 20H; CH$_2$O, *Z*), 2.93 (t, 4H; SCH$_2$, *Z*), 2.91 (m, 4H; SCH$_2$, *E*), 2.41 (s, 6H; SCH$_3$, *E*), 2.40 (s, 6H; SCH$_3$, *Z*); ^{13}C NMR (125.7 MHz, CDCl$_3$, 25°C, TMS): δ = 132.4 (*E*), 131.6 (*Z*), 126.2 (*E*), 125.8 (*Z*), 112.5 (*E*), 112.2 (*Z*), 72.0 (*E*), 71.9 (*Z*), 71.85 (*Z*), 71.8 (*Z*), 71.73 (*E*), 71.72 (*E*), 71.71 (*E*), 71.7 (*Z*+*E*), 71.2 (*Z*), 36.5 (*E*), 36.3 (*Z*), 20.2 (*Z*+*E*); MS (EI): [*M*]$^+$ calcd: 605.9859; found: 605.9840; elemental analysis calcd (%) for C$_{20}$H$_{30}$O$_5$S$_8$: C 39.60, H 4.99, O 13.25, S 42.21; found C 39.27, H 4.87, O 13.54, S 42.60.

Crystallographic data (excluding structure factors) for the structures reported in this paper have been deposited with the Cambridge Crystallographic Data Centre as supplementary publication no. CCDC-143693, CCDC-143694, CCDC-143695. Copies of the data can be obtained free of charge on application to CCDC, 12 Union Road, Cambridge CB2 1EZ, UK (Fax: (+44) 1223 336033; E-mail: deposit@ccdc.cam.ac.uk).

[1] For reviews related to this topic see, for example: a) S. Shinkai in *Comprehensive Supramolecular Chemistry*, Vol. 1 (Eds.: J. L. Atwood, J. E. Davies, J.-M. Lehn, D. D. MacNicol, F. Vögtle), Pergamon, Oxford, **1996**, pp. 671 – 700; b) A. E. Kaifer, S. Mendoza in *Comprehensive Supramolecular Chemistry*, Vol. 1 (Eds.: J. L. Atwood, J. E. Davies, J.-M. Lehn, D. D. MacNicol, F. Vögtle), Pergamon, Oxford, **1996**, pp. 701 – 732; c) P. L. Boulas, M. Gómez-Kaifer, L. Echegoyen, *Angew. Chem.* **1998**, *110*, 226; *Angew. Chem. Int. Ed.* **1998**, *37*, 216; d) P. D. Beer, P.A. Gale, G. Z. Chen, *J. Chem. Soc. Dalton Trans.* **1999**, 1897; e) L. M. Goldenberg, M. R. Bryce, M. C. Petty, *J. Mater. Chem.* **1999**, *9*, 1957.

[2] P. D. Beer, P. A. Gale, G. Z. Chen, *Coord. Chem. Rev.* **1999**, *185 – 186*, 3.

[3] a) T. K. Hansen, T. Jørgensen, P. C. Stein, J. Becher, *J. Org. Chem.* **1992**, *57*, 6403; b) R. Dieing, V. Morisson, A. J. Moore, L. M. Goldenberg, M. R. Bryce, J. M. Raoul, M. C. Petty, J. Garin, M. Saviron, I. K. Lednev, R. E. Hester, J. N. Moore, *J. Chem. Soc. Perkin Trans. 2* **1996**, 1587; c) F. Le Derf, M. Sallé, N. Mercier, J. Becher, P. Richomme, A. Gorgues, J. Orduna, J. Garin, *Eur. J. Org. Chem.* **1998**, 1861; d) F. Le Derf, M. Mazari, N. Mercier, E. Levillain, P. Richomme, J. Becher, J. Garín, J. Orduna, A. Gorgues, M. Sallé, *Inorg. Chem.* **1999**, *38*, 6096; e) F. Le Derf, M. Mazari, N. Mercier, E. Levillain, P. Richomme, J. Becher, J. Garín, J. Orduna, A. Gorgues, M. Sallé, *Chem. Commun.* **1999**, 1417; f) H. L. Liu, S. Liu, L. Echegoyen, *Chem. Commun.* **1999**, 1493; g) B. Johnston, L. M. Goldenberg, M. R. Bryce, R. Kataky, *J. Chem. Soc. Perkin Trans. 2* **2000**, 189; h) M. R. Bryce, A. S. Batsanov, T. Finn, T. K. Hansen, J. A. K. Howard, M. Kamenjicki, I. K. Lednev, S. A. Asher, *Chem. Commun.* **2000**, 295; i) M. Brøndsted, J. Becher, *Liebigs Ann.* **1997**, 2177; j) M. R. Bryce, *J. Mater. Chem.* **2000**, *10*, 589; k) M. Brøndsted Nielsen, C. Lornholt, J. Becher, *Chem. Soc. Rev.* **2000**, *29*, 153; l) F. Le Derf, E. Levillain, G. Trippé, A. Gorgues, M. Sallé, R.-M. Sebastían, A. M. Caminade, J.-P. Majoral, *Angew. Chem.*, in press.

[4] J. P. Lowe, *J. Am. Chem. Soc.* **1980**, *102*, 1262.

[5] a) T. K. Hansen, T. Jørgensen, F. Jensen, P. H. Thygesen, K. Christiansen, M. B. Hursthouse, M. E. Harman, M. A. Malik, B. Girmay, A. E. Underhill, M. Begtrup, J. D. Kilburn, K. Belmore, P. Roespstorff, J. Becher, *J. Org. Chem.* **1993**, *58*, 1359; b) J. Becher, T. K. Hansen, N. Malhotra, G. Bojesen, S. Bøwadt, K. S. Varma, B. Girmay, J. D. Kilburn, A. E. Underhill, *J. Chem. Soc. Perkin Trans. 1* **1990**, 175.

[6] J. Becher, J. Lau, P. Leriche, P. Mørk, N. Svenstrup, *J. Chem. Soc. Chem. Commun.* **1994**, 2715.

[7] a) J. Dale, P. O. Kristiansen, *Acta Chem. Scand.* **1971**, *26*, 1471;
     b) H. M. Li, B. Post, H. Morawetz, *Makromol. Chem.* **1972**, *154*, 89.

[8] A. Souizi, A. Robert, P. Batail, L. Ouahab, *J. Org. Chem.* **1987**, *52*,
     1610.

[9] A fully aliphatic S(CH$_2$)$_{12}$S bridge was shown to let the TTF skeleton
     be essentially planar: K. Boubekeur, C. Lenoir, P. Batail, R. Carlier,
     A. Tallec, M. P. Le Paillard, D. Lorcy, A. Robert, *Angew. Chem.* **1994**,
     106, 1448; *Angew. Chem. Int. Ed. Engl.* **1994**, *33*, 1379.

[10] The cavity size is defined by d(O1-O4) $\times$ ($\frac{1}{2}$[d(O3−S3) + d(O2−S1)])
     for (*Z*)-**2**, and d(O1−O5) $\times$ ($\frac{1}{2}$[d(O3−S1) + d(O3−S3)]) for (*Z*)-**3**
     (crystallographic numeration).

[11] G. Bonas, C. Bosso, M. R. Vignon, *Rapid. Commun. Mass Spectrom.*
     1988, *2*, 88.

[12] R. D. Shannon, *Acta Crystallogr.* **1976**, *32*, 751.

[13] M. J. Hynes, *J. Chem. Soc. Dalton Trans.* **1993**, 311.

[14] a) H. A. Benesi, J. H. Hildebrand, *J. Am. Chem. Soc.* **1949**, *71*, 2703;
     b) H. Tsukube, H. Furuta, A. Odani, Y. Takeda, Y. Kudo, Y. Inoue, Y.
     Liu, H. Sakamoto, K. Kimura in *Comprehensive Supramolecular*
     Chemistry, *Vol.* 8 (Eds.: J. L. Atwood, J. E. Davies, J.-M. Lehn, D. D.
     MacNicol, F. Vögtle), Pergamon, Oxford, **1996**, pp. 425 – 482.

[15] M. Rudolph, D. P. Reddy, S. W. Feldberg, *Anal. Chem. A* **1994**, *66*, 589.

[16] a) J. M. Williams, J. R. Ferraro, R. J. Thorn, K. D. Carlson, U. Geiser,
     H. H. Wang, A. M. Kini, M. H. Whangbo, *Organic Superconductors*
     (Including Fullerenes). Synthesis, Structure, Properties and Theory,
     Prentice Hall, New Jersey, **1992**; b) G. Saito, *Pure Appl. Chem.* **1987**,
     59, 999; c) E. B. Yagubskii, *Mol. Cryst. Liq. Cryst.* **1993**, *230*, 631.

[17] a) C. J. Gomez-Garcia, L. Ouahab, C. Gimenez-Saiz, S. Triki, E.
     Coronado, P. Delhaes, *Angew. Chem.* **1994**, *106* 234; *Angew. Chem.*
     Int. Ed. Engl. **1994**, *33*, 223; b) M. Kurmoo, A. W. Graham, P. Day, S. J.
     Coles, M. B. Hursthouse, J. L. Caulfield, J. Singleton, F. L. Pratt, W.
     Hayes, L. Ducasse, P. Guionneau, *J. Am. Chem. Soc.* **1995**, *117*,
     12209 – 12217; c) E. Coronado, J. R. Galán-Mascarós, C. J. Gómez-
     Garcia *J. Chem. Soc. Dalton Trans.* **2000**, 205.